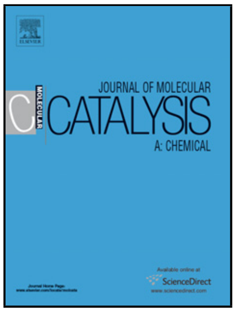

Title: Immobilization of copper nanoparticles on perlite: Green synthesis, haracterization and catalytic activity on aqueous reduction of 4-nitrophenol

Author: Mahmoud Nasrollahzadeh S.Mohammad Sajadi
Akbar Rostami-Vartooni Mojtaba Bagherzadeh Reza Safari

PII: S1381-1169(15)00047-3
DOI: http://dx.doi.org/doi:10.1016/j.molcata.2015.01.032
Reference: MOLCAA 9415

To appear in: *Journal of Molecular Catalysis A: Chemical*

Received date: 12-12-2014
Revised date: 29-1-2015
Accepted date: 30-1-2015

Please cite this article as: Mahmoud Nasrollahzadeh, S.Mohammad Sajadi, Akbar Rostami-Vartooni, Mojtaba Bagherzadeh, Reza Safari, Immobilization of copper nanoparticles on perlite: Green synthesis, haracterization and catalytic activity on aqueous reduction of 4-nitrophenol, Journal of Molecular Catalysis A: Chemical http://dx.doi.org/10.1016/j.molcata.2015.01.032

Immobilization of copper nanoparticles on perlite: Green synthesis, characterization and catalytic activity on aqueous reduction of 4-nitrophenol

Mahmoud Nasrollahzadeh,[*,a] S. Mohammad Sajadi,[b] Akbar Rostami-Vartooni,[a] Mojtaba Bagherzadeh[c] and Reza Safari[a]

[a]*Department of Chemistry, Faculty of Science, University of Qom, Qom 3716146611, Iran*

[b]*Department of Petroleum Geoscience, Faculty of Science, Soran University, PO Box 624, Soran, Kurdistan Regional Government, Iraq*

[c]*Material Research School, NSTRI, 81465-1589, Isfahan, I. R. Iran*

ABSTRACT

We report the facile synthesis of environmentally benign Cu NPs/perlite composites without employing any toxic reductants or capping agents. Renewable natural *Euphorbia esula L.* not only functioned as a reductant, but also served as a stabilizer for the formation of Cu NPs. Cu NPs synthesized using aqueous extract of the leaves of *Euphorbia esula L.* was immobilized on perlite by a very simple and inexpensive method. The structural investigation was performed using XRF, XRD, SEM, EDS, TEM, TG-DTA, BET and FT-IR. The Cu NPs/perlite shows favorable activity and separability on the catalytic reduction of 4-nitrophenol, and can be reused several times without a decrease in the catalytic activity. Their reaction rate constant was calculated according to the pseudo-first-order reaction equation.

Keywords: Green synthesis; Perlite; Copper nanoparticles; Reduction; 4-Nitrophenol

1. Introduction

The homogeneous Cu catalyst is known as one of the most efficient catalytic systems for various organic reactions [1-4]. However, homogeneous catalysts suffer from certain disadvantages such as metal aggregation and precipitation which cause catalyst decomposition and a considerable loss of catalytic activity, and are difficult to purify and reuse after chemical reactions which leads to a loss of expensive metal and ligands and contamination to the products [1-4]. Catalyst separation is a critically important issue, and catalysts that are active but difficult to recycle/recover from the reaction mixture are generally not preferred in the chemical industry.Thus, the use of heterogeneous copper catalysts is often desirable from the perspective of process development due to their easy handling, simple recovery, and recycling.

Since catalysis takes place on metal surface, nanoparticles (NPs) are much more reactive than the particulate metal counterpart due to their small sizes and large surface areas [5]. So, heterogeneous catalysts are more and more used in the form of nanoparticles. Unfortunately, the agglomeration of metal NPs is inevitable due to their small size, resulting in a remarkable reduction in their catalytic activities [6]. To prevent the agglomeration of metal nanoparticles (MNPs) and the over-stoichiometric use of Cu reagents, the catalytically active metal NPs are usually immobilized on/into less expensive solid supports such as polymers, carbon, metal oxides, grapheme, gum and zeolite regarded as ideal supports for heterogeneous catalyst due to their excellent stability, high surface area, tunable pore size, and robust surface chemistry [2-4,7-11]. However, most of these supports suffer from inefficiency to achieve highly distributed and stable noble metal NPs. Therefore, it is desirable to develop an efficient and new support for the immobilization of metal NPs.

Perlite is a naturally occurring dense glassy volcanic rock and can be expanded up to 10-20 times its original volume when heated rapidly at 700-1200 °C [12]. Perlite is generally chemically inert and has a pH of approximately 7. It contains silica (greater than 70%), aluminum, potassium, sodium and 3-5% water and is used filler in various processes such as paint, enamels, glazes, plastics, and resins [13]. Since perlite granules are highly porous media, they can naturally act as an excellent support. So far of our knowledge, there is no report of using of perlite as a support for the preparation of new catalysts. This study considers perlite could be used as a support for the immobilization of copper NPs. The purpose of this study was to evaluate the catalytic activity of Cu NPs/perlite composites for reduction of 4-nitrophenol in water. Copper (Cu) is relatively cheap compared to other noble metals such as gold (Au), palladium (Pd) and platinum (Pt).

2. Experimental

2.1. Instruments and reagents

High-purity chemical reagents were purchased from the Merck and Aldrich chemical companies. All materials were of commercial reagent grade. Melting points were deter-mined in open capillaries using a BUCHI 510 melting point apparatus and are uncorrected. ^{1}H NMR and ^{13}C NMR spectra were recorded on a Bruker Avance DRX spectrometer at 400 and 100 MHz, respectively. The element analyses (C, H, N) were obtained from a Carlo ERBA Model EA 1108 analyzer carried out on Perkin-Elmer 240c analyzer. X-Ray diffraction (XRD) was performed at 25 °C (D/Max-2550 PC, RIGAKU, Japan) in reflection mode using Cu Ka radiation. Fourier transform infrared (FT-IR) spectra were recorded using a Nicolet 5700 spectrometer (Thermo Nicolet Corporation, US) at the wavenumber range 4000-400 cm^{-1} at ambient conditions. Morphologies of catalyst were observed using a scanning electron microscope (JSM-5600LV, JEOL Ltd., Japan) with an operating voltage of 15 kV. The elemental composition of catalyst was analyzed using an X-ray energy dispersive spectroscopy (EDS) detector (IE 300X, Oxford, UK) attached to the SEM. Thermogravimetric-differential thermal analysis (TG-DTA) was performed using STA 1500 Rheometric Scientific (England). The flow rate of air was 120 ml/min and the ramping rate of sample was 2 ^{o}C/min. The shape and size of Cu NPs crystals were identified by transmission electron microscope (TEM) using a Philips EM208 microscope operating at an accelerating voltage of 90 kV. The Brunauer-Emmett-Teller (BET) specific surface areas (SBET) and the porosity of the samples were evaluated on the basis of nitrogen adsorption isotherms measured at 77 K using a BELSORP-max nitrogen adsorption apparatus (Japan Inc.). Ultraviolet-visible (UV-vis) absorption spectra were recorded by a Shimadzu UV 2100 PC UV-visible spectrophotometer.

2.2. Preparation of extract of the leaves of Euphorbia esula L.

50 g of dried powder of the leaves of *Euphorbia esula L.* was extracted using boiling in 300 mL double distillated water for 20 min and aqueous extract was centrifuged in 7000 rpm to obtain the supernatant as extract [14]. According the literatures, the most important phytochemicals inside this genus are mainly terpenoids, flavonoids, phenolic acids, tannins, sterols, skin-irritating and tumor promoting latexes and also their active ingenol diterpenoids in different parts of the plant [15-17].

2.3. Green synthesis of copper nanoparticles using Euphorbia esula L. leaves extract

The copper nanoparticles were synthesized by the following process. In a 250 mL conical flask, 10 mL solution of $CuCl_2 \cdot 2H_2O$ 5 mM was mixed with 100 mL of the aqueous plant extract (100 g dried leaves of the plant extracted using 500 mL of deionized water while heating at 80 °C and pH 9 for 30 min then filtered) along with vigorous shaking until gradually changing the color of the mixture during 20 min from yellow to dark indicating the formation of Cu nanoparticles (as monitored by UV-vis and FT-IR spectra of the solution). The well shaked mixture then filtered and centrifuged at 6500 rpm for 30 min and obtained precipitation washed with absolute ethanol and double distillated water, respectively. Then, the nano zero valent copper was calcined at 600 ˚C [14].

2.4. Preparation of Cu NPs/perlite

The Cu NPs/perlite was fabricated by immobilization of Cu NPs synthesized using aqueous extract of the leaves of *Euphorbia esula L* on perlite. Approximately, 1.0 g of perlite was dispersed in 15 mL of an aqueous Cu NPs solution (0.05 M) and stirred for 15 h at 100 ˚C. Then, the mixture was cooled down to room temperature, filtered, washed with water, and dried.

2.5. Reduction of 4-nitrophenol by Cu NPs/perlite

A 0.25 M solution of freshly prepared $NaBH_4$ (25 mL) was added to the stirred mixture of 2.5 mM 4-nitrophenol solution (25 mL) and 10 mg of the Cu NPs/perlite catalyst. The mixture was stirred at room temperature until the deep yellow solution became colorless. The reaction progress was monitored by UV-vis spectroscopy at a wavelength of 400 nm. 1.0 mL of the solution was extracted and diluted to 25 mL for further UV-vis absorption analysis at certain intervals. After completion of reaction, the catalyst was simply separated by simple filtration and washed successively with ethanol and water, and then dried and was used for successive cycles. The product was confirmed by their melting points and ^1H NMR spectroscopy.

3. Results and discussion

Most of the routes for the synthesis of metal nanoparticles use chemical reduction routes which pose high environmental risk because of chemical toxicity and biological hazards. The green synthesis techniques are generally synthetic routes that utilize relatively nontoxic solvents such as water, biological extracts, and biological systems [18,19]. Due to our ongoing interest on the green synthesis of metal NPs [20-23], we wish to report a new and rapid protocol for preparation of Cu NPs by using *Euphorbia esula L.* [24,25] leaf extract as a reducing and stabilizing agent.

The *Euphorbia esula L.* [24,25] leaf extract which is rich in terpenoids, flavonoids, tannins, sterols and other aromatic compounds may possibly responsible for reduction of Cu^{2+} metal ions and effective stabilization of synthesized NPs. Of course the formation of copper NPs is mainly affected using the reduction of metal ions by antioxidant constituents such as flavonoids present in the extract of the leaves of *Euphorbia esula L.* to nano zero valent (NZV) metallic particles (Figure 1).

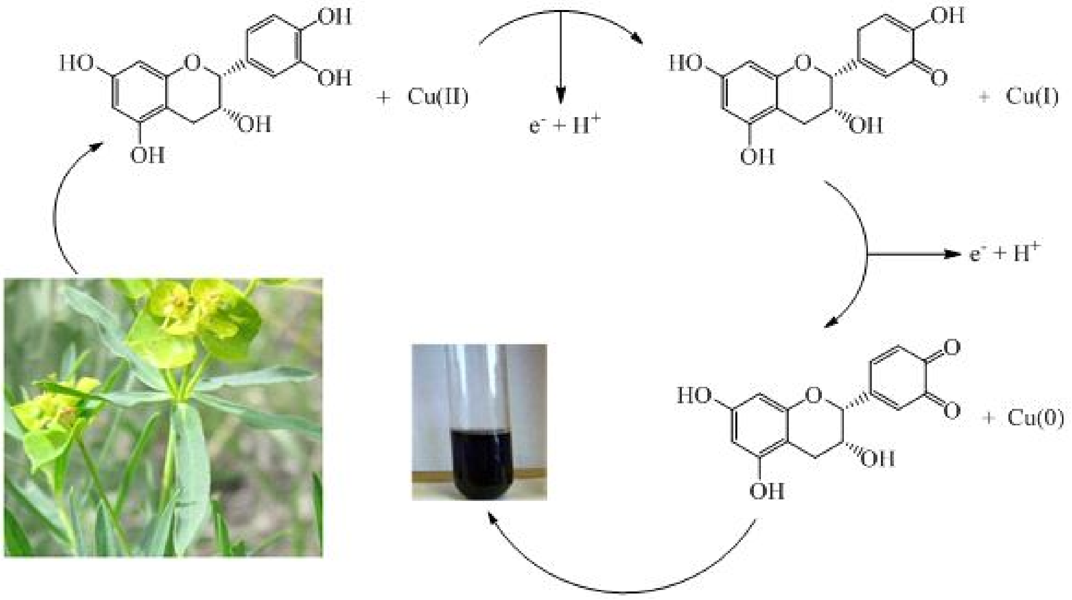

Figure 1. Bioreduction of metallic ions using the flavonoids as potent antioxidants in aqueous extract of the leaves of *Euphorbia esula L.*

The synthesized nanoparticles have been well characterized by XRD, TEM and UV-vis spectroscopy [14].

UV-vis spectroscopy is an important technique to determine the formation and stability of metal NPs in aqueous solution. Figure 2 shows the UV-vis spectra of Cu NPs formation. Our results showed that the maximum absorbance of green synthesized Cu NPs was at 580 nm due to the surface plasmon absorption of nanosized Cu particles.

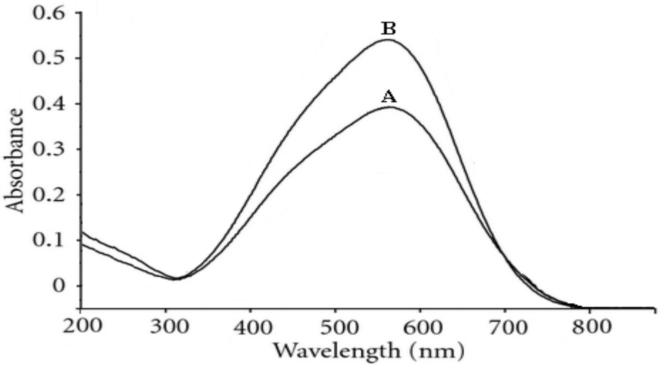

Figure 2. UV-vis spectrum of Cu NPs synthesized using aqueous extract of the leaves of *Euphorbia esula L*) .A; 20 min and B; 30 min.(

The Cu NPs/perlite was prepared by a simple procedure, via the immobilization of Cu NPs synthesized using aqueous extract of the leaves of *Euphorbia esula L.* and was thoroughly characterized by various sophisticated analytical techniques such as XRF, XRD, SEM, EDS, TEM, TG-DTA, FT-IR and BET specific surface area studies.

The chemical compositions of the perlite were determined with XRF (Table 1). It is noteworthy that the perlite is a natural alumino-silicate; rich in SiO_2 and Al_2O_3.

Table 1

Typical approximate composition analysis of perlite.

Constituent	Typical, %
SiO_2	60-75
Al_2O_3	12-16
Na_2O	5-10
K_2O	2-5

CaO	0-2
MgO	0-1
Fe_2O_3	0-1
Combined H_2O	1-2

The FT-IR spectra of Cu NPs/perlite is shown in Figure 3, the broad peak around 3400 cm^{1-} indicates the O-H bond vibrations. An O-H deformation vibration was observed near 1630 cm.$^{1-}$ The remaining peaks at 1355, 1035, 782, and 453 cm^{1-} correspond to the stretching bands of Si-O and Si-O-Si groups, and deformation bands of Si-O group and Al-O-Si groups of perlite, respectively. The FT-IR studies of Cu NPs/perlite confirm that there was no change in functional group after the immobilization of Cu NPs on perlite.

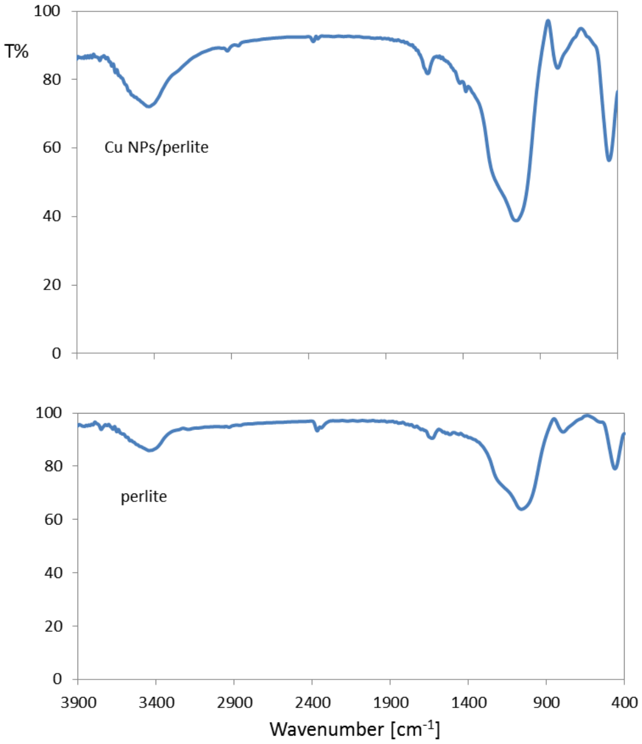

Figure 3. FT-IR spectrum of Cu NPs/perlite and perlite.

Figure 4 shows the XRD pattern of Cu NPs/perlite. The broad peak centered at 2θ = 25° was assigned to the characteristic peak of perlite, indicating its amorphous nature. Notably, no reflections assignable to metallic Cu were present in the XRD pattern of Cu NPs/perlite, possibly due to the poor crystallinity of the Cu particles in Cu NPs/perlite. In order to confirm the presence of a metallic Cu component in Cu NPs/perlite, the chemical composition of the products was further analyzed by the

Energy Dispersive X-ray Spectroscopy (EDS) spectrum. It further confirmed that Cu NPs/perlite was composed of Si, Al, Cd, Fe, Cu and oxygen (Figure 5).

The size and shape of the Cu NPs/perlite was examined by scanning electron microscopy (SEM) and transmission electron microscopy (TEM). Figure 5 shows typical large-scale FE-SEM images of the as-produced Cu NPs/perlite. It is clearly observed that the Cu NPs have various sizes less than 32 nm.

The size of as-prepared Cu NPs/perlite was further examined by TEM (Figure 5). The particles exhibited spherical morphology with low tendency to agglomeration.

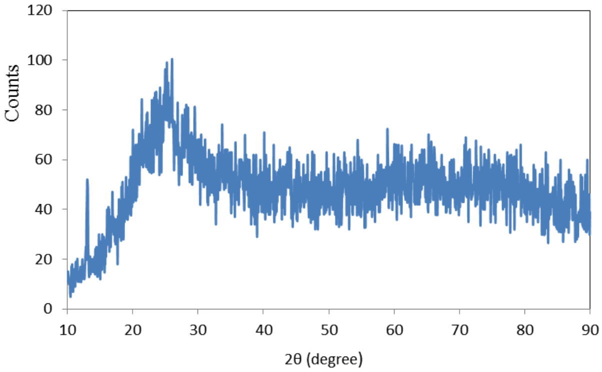

Figure 4. XRD powder pattern of Cu NPs/perlite.

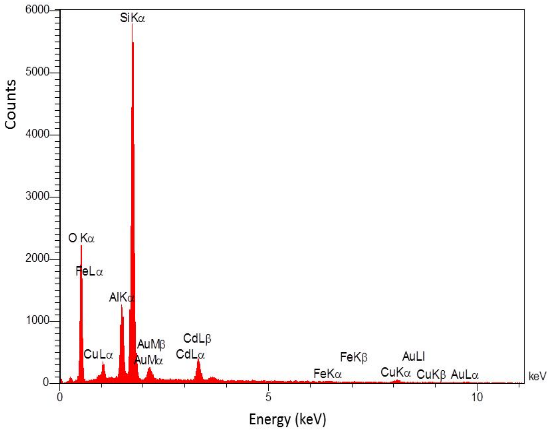

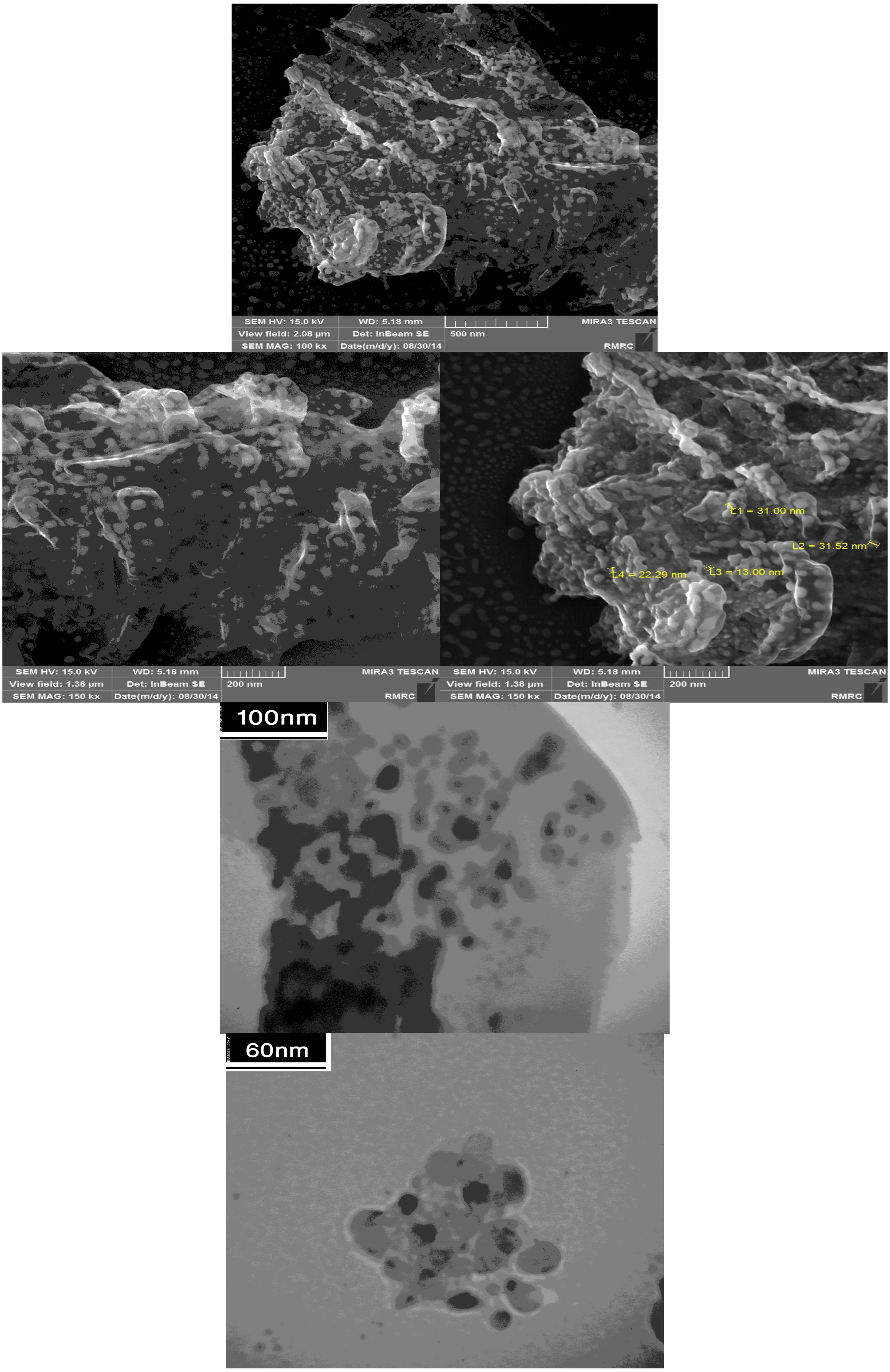

Figure 5. EDS spectrum, FE-SEM and TEM images of Cu NPs/perlite.

The specific surface areas and pore volume of Cu NPs/perlite was determined by BET (Brunauer-

Emmett-Teller). The N_2 adsorption-desorption isotherm and Barrett-Joyner-Halenda (BJH) pore size distribution plot of Cu NPs/perlite showed in Figure 6. The results indicate that the specific surface area, pore volume, and average pore diameter of perlite were increased after immobilization of copper nanoparticles. Based on isotherm curve, the measured BET surface area of Cu NPs/perlite was 3.8 m^2/g, whereas the surface area of perlite is 1.73 m^2/g [26]. It is clear that number of pores on the surface of perlite fairly increased after immobilization of copper nanoparticles. Moreover, the Barrett-Joyner-Halenda (BJH) analysis showed that the average pore diameter is 8.1 nm and the pore volume is 7.7×10^{-3} cc/g, whereas the average pore diameter and pore volume of perlite is 1.9 nm and 2.29×10^{-3} cc/g, respectively [26].

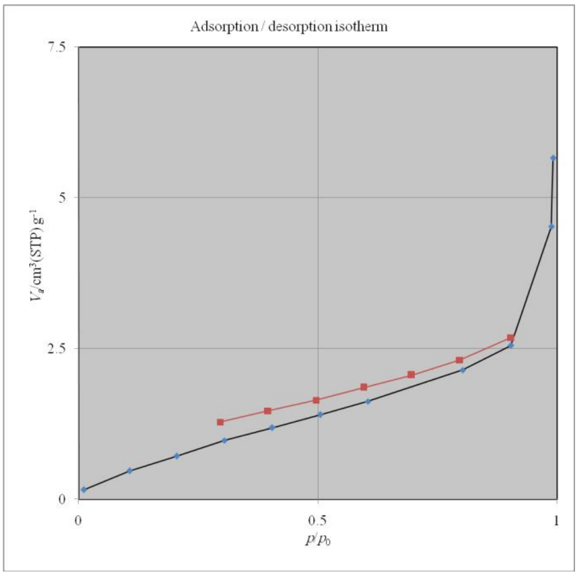

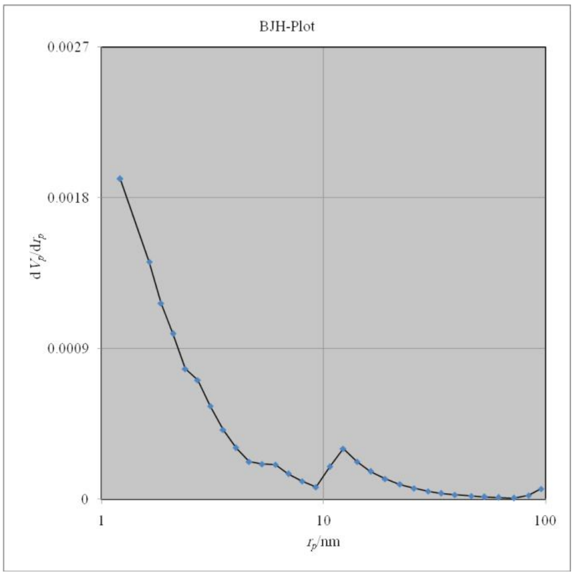

Figure 6. The N_2 adsorption-desorption isotherm and Barrett-Joyner-Halenda (BJH) pore size distribution plot of catalyst.

Figure 7 shows the TG/DTA curves measured for Cu NPs/perlite. In the TG/DTA data of Cu NPs/perlite a gradual weight decreasing (about 4.0 wt %) was only observed between 180 and 300 °C corresponding to desorption of surface water.

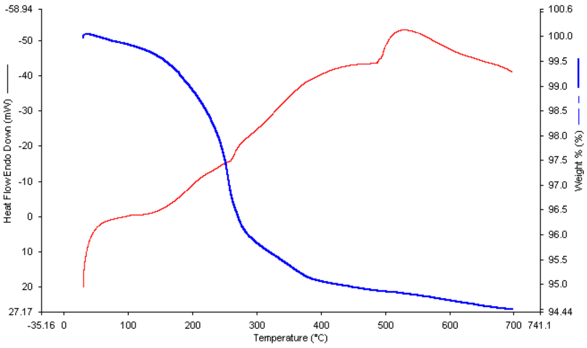

Figure 7. TG/DTA data measured for Cu NPs/perlite.

Evaluation of the catalytic activity of Cu NPs/perlite through the reduction of 4-nitrophenol in water

4-Nitrophenol (4-NP) is carcinogenic and genotoxic to human beings and wildlife, which can damage the central nervous system, liver, kidney and blood of humans and animals. Degradation of the compound to nondangerous product is difficult because of its high stability and low solubility in water [27]. The reduction or conversion of 4-NP acquires great importance both environmentally and industrially. Its reduction product, 4-aminophenol (4-AP), is an important industrial intermediate for manufacturing analgesic and antipyretic drugs, anticorrosion lubricants, and hair dying agents [28]. Therefore, developing an efficient, durable and eco-friendly method to produce 4-AP is a major challenge in catalysis research. The reduction of 4-NP with sodium borohydride ($NaBH_4$) as reducing agent in the presence of Cu NPs has been extensively investigated in our previous work [29]. However, the catalytic performance of Cu NPs/perlite in the reduction of 4-NP to 4-AP has not been well examined. In the present work, the catalytic performance of the synthesized Cu NPs/perlite was evaluated by the reduction of 4-NP with $NaBH_4$ to 4-AP (Scheme 1).

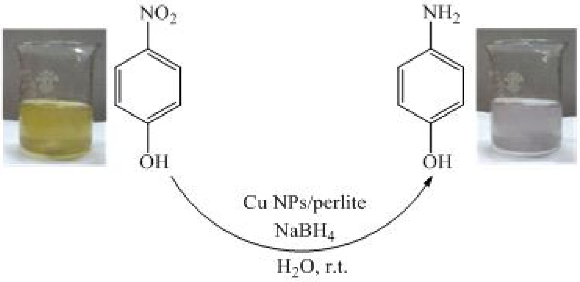

Scheme 1. The reduction of 4-NP on the surface of Cu NPs/perlite catalyst.

The UV-vis spectra of the reaction mixture were monitored with the progress of the catalytic reduction of 4-NP (Figure 8a and 8b). As shown in Figure 8, there was a red shift of the peak of 4-NP from 317 to 400 nm, observed immediately after the addition of $NaBH_4$. This was due to the formation of 4-nitrophenolate ions under alkaline conditions caused by the addition of $NaBH_4$ (Scheme 2) [30]. The absorption of 4-NP at 400 nm decreases with a concomitant increase in the peak at about 300 nm, which is attributed to the reduced product, 4-aminophenol. The absorption peak at 400 nm is fully disappeared after about 2.5 min in the presence of 10 mg of Cu NPs/perlite catalyst. Without catalyst, no significant color change was observed within the reaction time and the peak at 400 nm remained unaltered for a long duration. This suggests that even an excessive concentration of $NaBH_4$ cannot reduce 4-nitrophenolate ions completely in the absence of catalysis. Also, the loss of catalytic activity was not observed after the catalyst was recycled for three times, indicating high stability of the Cu NPs/perlite catalyst.

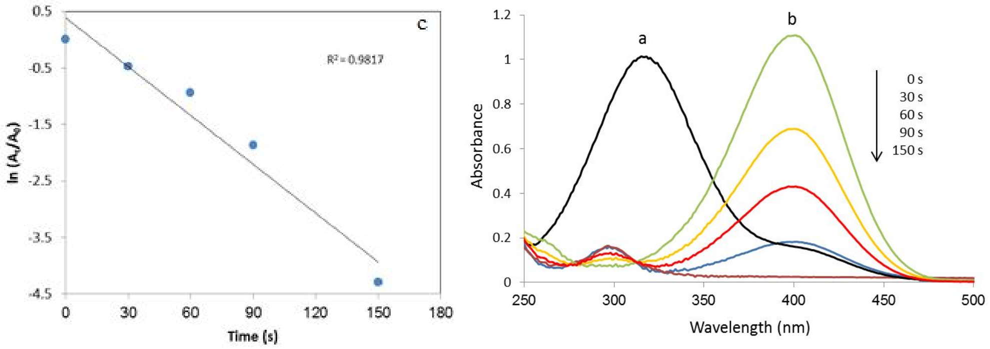

Figure 8. (a) UV-visible spectra of 4-NP in the absence of $NaBH_4$, (b) Time-dependent UV-visible absorption spectra for the reduction of 4-NP, Conditions: [4-NP] = 2.5×10^{-3} M; [$NaBH_4$] = 0.25 M; catalyst = 10 mg, (c) Plot of $\ln(A_t/A_0)$ versus time for the reduction of 4-NP with Cu/perlite. Conditions: [4-NP] = 2.5×10^{-3} M; [$NaBH_4$] = 0.25 M; catalyst = 10 mg.

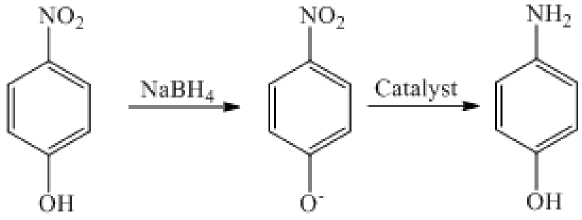

Scheme 2. The reduction reaction for the conversion of 4-NP to 4-AP.

Due to the presence of large excess of $NaBH_4$ compared to 4-NP, the rate of reduction is independent of the concentration of $NaBH_4$, and the reduction of 4-NP to 4-AP can be treated as a pseudo-first-order reaction. As the absorbance of 4-NP is proportional to its concentration in the medium, the ratio of A_t/A_0 is proportional to the ratio of C_t/C_0 (A_t is the absorbance at any time t, A_0 is the absorbance at time t = 0, C_t is the concentration of 4-NP in the reaction time t and C_0 is the initial concentration of 4-NP). Pseudo-first-order rate constant could be calculated by the following rate law equation [31]:

$$\ln(C_t/C_0) = \ln(A_t/A_0) = -kt$$

where, k is the rate constant. From the linear relations of $\ln(A_t/A_0)$, shown in Figure 8c, we found that the rate constant for this reaction is 0.027 s^{-1}, which is comparable to those reported previously [32,33].

To show the advantages of proposed method in comparison with other reported methods, we summarized some of results for reduction of 4-NP in Table 2, which shows that Cu NPs/perlite is an equally or more efficient catalyst with respect to reaction time and yield than previously reported ones.

Compared with the other literature works on the reduction of 4-NP, the notable features of our method are:

- The reaction system is clean;
- Elimination of toxic reagents and homogeneous catalysts;
- The conversion and yield of the product is very high;
- The use of plant extract as an economic and effective alternative represents an interesting, fast and clean synthetic route for the large scale synthesis of Cu NPs;
- Avoidance of the high reaction temperature;
- Natural and highly efficient heterogeneous catalyst activity;
- Ease of handling and cost efficiency of the catalyst;
- Avoidance of the non-green solvents application and by-products preparation;
- Higher yields and purity, shorter reaction time and milder conditions;
- The Cu NPs/perlite can be easily recovered.

Table 2

Comparison present methodology with other reported methods in the reduction of 4-NP.

Entry	Conditions (yield, %)	Ref.
1	GA-Pt NPs, H_2O, H_2, r.t., 8 h (82)	34
2	Resin-Au NPs, MeOH/H_2O, $NaBH_4$, 40 °C, 20 min (82)	35
3	NAP-Mg-Au(0), H_2O, $NaBH_4$, r.t., N_2, 7 min (98)	36
4	Ni-PVAm/SBA-15, H_2O, $NaBH_4$, r.t., 85 min (98)	37
5	TiO_2-$G_{1\%}$,H_2O, oxalic acid, ultraviolet light (16W), N_2, 60 min (95)	38
6	Fe_3O_4@C@Pt, EtOH, H_2, r.t., 60 min (98)	39
7	Cu NPs, THF/H_2O, $NaBH_4$, 50 °C, 2 h (66)	40

8	HMMS-NH$_2$-Pd, EtOH, H$_2$, r.t., 60 min (98)	41
9	Polymer-anchored Pd(II) complex, DMF, H$_2$, 30 °C, 5.5 h (84)	42
10	PdCu/graphene, EtOH/H$_2$O, NaBH$_4$, 50 °C, 1.5 h (98)	43
11	KCC-1/Au, H$_2$O, NaBH$_4$, r.t., 12 min	44
12	Au-GO, H$_2$O, NaBH$_4$, r.t., 30 min	45
13	Au/graphene hydrogel, H$_2$O, NaBH$_4$, r.t., 720 s	46
14	Au@PZS@CNTs, H$_2$O, NaBH$_4$, r.t., 16 min	47
15	Ag/KCC-1, H$_2$O, NaBH$_4$, r.t., 510 s	48
16	Cu NPs, H$_2$O, NaBH$_4$, r.t., 50 min	49
17	Pd-FG, H$_2$O, NaBH$_4$, r.t., 12 min	50
18	p(AMPS)-Ni composite, H$_2$O, NaBH$_4$, 30 °C, 60 min	51
19	p(AMPS)-Co composite, H$_2$O, NaBH$_4$, 30 °C, 28 min	52
20	Cu NPs/perlite, H$_2$O, NaBH$_4$, r.t., 2.5 min (99)	This work

It is important to point out that the Cu NPs/perlite composites show relatively higher catalytic activity than Cu NPs alone. We investigated the effects of the perlite support on the catalytic activity. Reduction of 4-NP with NaBH$_4$ was carried out respectively in the absence of a catalyst, the presence of Cu NPs, the presence of perlite, and the presence of Cu NPs/perlite composite to investigate the catalytic effect of the as-prepared Cu NPs/perlite on the reaction. According to the results, no appreciable reaction took place after 30 min without a catalyst or in the presence of perlite. A reaction time of 580 s was required to achieve the full reduction of 4-NP by NaBH$_4$ using Cu NPs alone as catalysts. But when the Cu NPs/perlite composite was used as the catalyst, the reaction proceeded much faster and completed in 2.5 min. Such observation indicates that the perlite support may play an active part in the catalysis, yielding a synergistic effect. The synergistically enhanced catalytic activity may be explained as follows: given that 4-NP is π-rich in nature, it is expected that 4-NP can be adsorbed onto perlite via π–π stacking interactions. Such adsorption provides a high concentration of 4-NP near to the Cu NPs on perlite, leading to highly efficient contact between them. In contrast, without a highly adsorbent perlite support, 4-NP must collide with Cu NPs by chance, and remains in contact for the catalysis to proceed. When this is not achieved, 4-NP will pass back into solution and can only react further when it collides with Cu NPs again [33].

Finally, the focus of on the experimental study of catalysis (such as Cu NPs/perlite) effects on immobilization of copper NPs on perlite, the obtained results can be demonstrated by computational studies, in which intra-molecular catalyst affects the nano-sized organic systems. As our current work we investigate the intra-molecular electronic transport mechanisms in organic systems, induced by surface/catalyst effect, using quantum theory of atoms-in-molecule (QTAIM). The QTAIM that can be utilized to determine the chemical behaviour of organic molecular systems as an expansion of quantum mechanics to proper the open molecular systems in terms of the topology of such systems or *local* electron density $\rho(r)$, Laplacian $\nabla^2\rho(r)$, atomic electronic energy E_{elec}, molecular Virial/potential force $V(r)$ and bonding characteristics [53-55]. Using the QTAIM, the contour maps of the electron density and its Laplacian and Virial force of the NO_2-Ph-OH, NO_2-Ph-O^-, NH_2-Ph-OH molecules and -C-NO_2-Cu-O- bonding plan, in the molecular planes are calculated and results demonstrated in Figures 9 and 10. Analysis of computational results (not reported here for brevity) shows that the oxygen atoms of the NO_2 functional group have different local electronic properties (such as electron density, atomic basins and atomic boundary surfaces). Also, atomic scale analyses of the results demonstrate that the hydrogen and carbon atoms of the rings are generally the weakest responses to catalyst nature and in which its effects on the NO_2 group is larger than OH functional group. It is also predicted that the interaction (or absorption) between nano-size Cu particles of the Cu NPs/perlite catalyst and NO_2 functional group of the molecule (-Cu-NO_2-) play a dominant role in the intra-molecular electronic transport for the reduction of NO_2. Moreover, it is possible to predict and study the *molecular/submolecular* energy and charge transfers to determine atoms and functional groups with lower or higher sensitivity to surface/catalyst effect as an important factor for effective designing the actual molecular systems and intelligent control of their environmental behaviour.

	$\rho(r)$
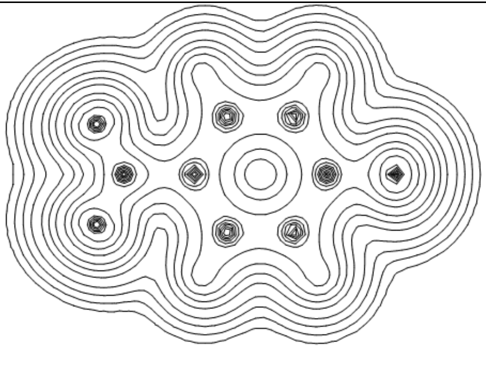	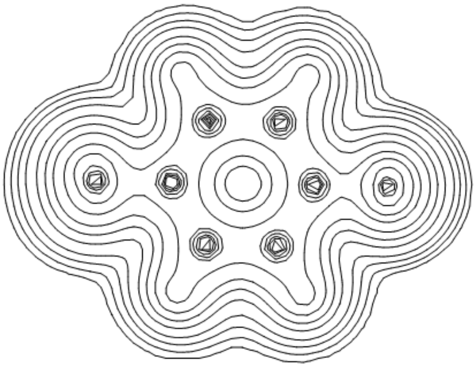
$\nabla^2\rho(r)$	

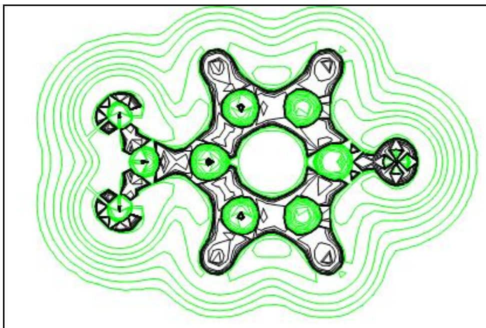	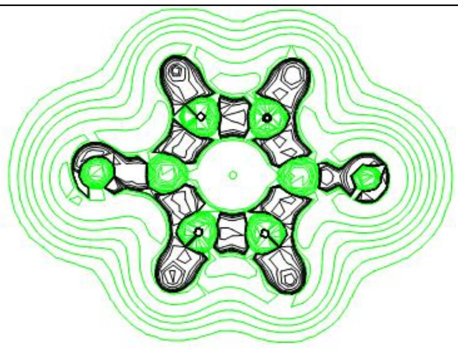
$V(r)$	
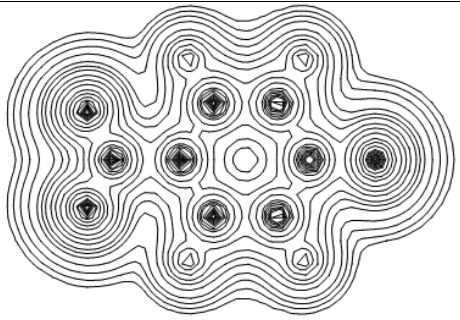	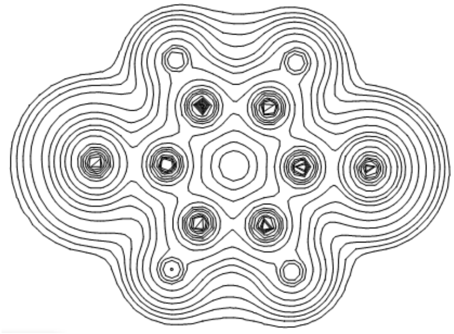
Figure 9. The contour maps of the electron density ($\rho(r)$) and its Laplacian ($\nabla^2\rho(r)$) and Virial force $V(r)$ of the NO$_2$-Ph-OH (left) and NH$_2$-Ph-OH (right) molecules, in the molecular planes, are calculated using QTAIM.	
	$\rho(r)$

<table>
<tr><td>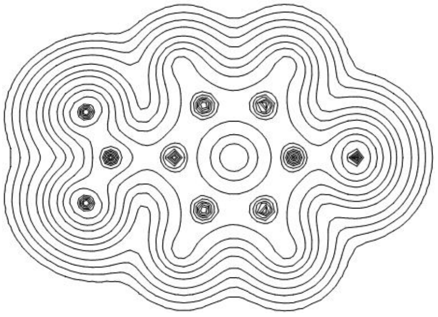</td><td>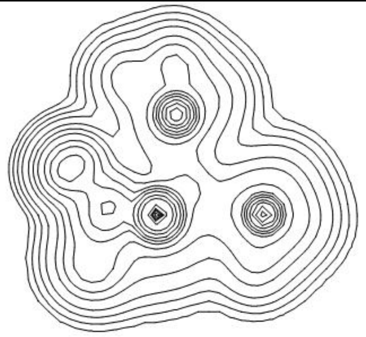</td></tr>
<tr><td colspan="2">$\nabla^2\rho(r)$</td></tr>
<tr><td>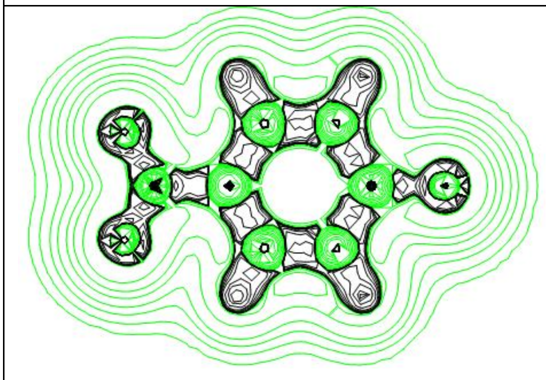</td><td>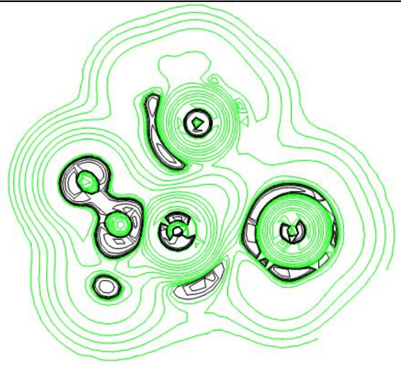</td></tr>
<tr><td colspan="2">$V(r)$</td></tr>
</table>

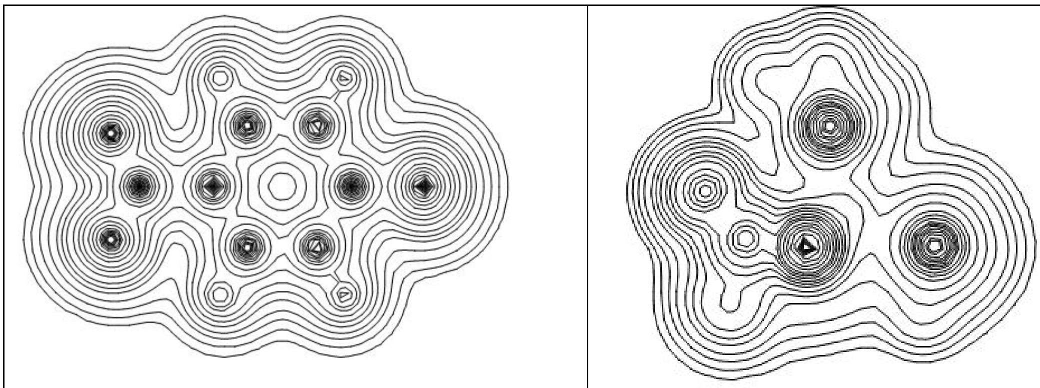

Figure 10. the contour maps of the electron density ($\rho(r)$) and its Laplacian ($\nabla^2\rho(r)$) and Virial force $V(r)$ of the NO_2-Ph-O^- (left) molecule and -C-NO_2-Cu-O- bonding plan (right), in the molecular planes, in the molecular planes, are calculated using QTAIM.

Catalyst recyclability

The reusability, which is an important factor for a catalyst, was investigated by recovering the Cu NPs/perlite catalyst from the reaction mixture by filtration and reusing it in the next reaction. The perlite supports not only enhance the catalytic activity of Cu NPs via a synergistic effect, but also lend the Cu NPs/perlite the easiness of separation and recovery for practical catalytic applications. After completion of the reaction, the catalyst was separated by simple filtration and was washed with ethanol and water, dried in a hot air oven at 100 °C for 2 h and the recycled catalyst was saved for the next round. The slight yield loss was observed after three cycles. Meanwhile, EDS observation after the repeated catalytic tests was also carried out to check the stability of the as-prepared catalyst. It was found that the Cu content of the Cu NPs/perlite was scarcely changed, suggesting the good stability of the materials.

4. Conclusions

In conclusion, Cu NPs/perlite with good catalytic activity has been successfully fabricated by immobilization of Cu NPs on perlite. Cu NPs was prepared using aqueous extract of the leaves of *Euphorbia esula L.* The as-prepared Cu NPs/perlite catalyst exhibits excellent catalytic activity and recyclability for the reduction of 4-NP to 4-AP. The rate constant and the reaction yield calculated for the reduction of 4-nitrophenol is comparable to the best reported in the literature.

Acknowledgments

We gratefully acknowledge the Iranian Nano Council and the University of Qom for the support of this work.

References

- M. Nasrollahzadeh, A. Ehsani, M. Maham, Synlett 25 (2014) 505.
- M. Nasrollahzadeh, A. Zahraei, A. Ehsani and M. Khalaj, RSC Adv. 4 (2014) 20351.
- M. Nasrollahzadeh, A. Rostami-Vartouni, A. Ehsani, M. Moghadam, J. Mol. Catal. A Chem. 387 (2014) 123.
- M. Nasrollahzadeh, M. Enayati, M. Khalaj, RSC Adv. 4 (2014) 26264.
- P. Fakhri, B. Jaleh, M. Nasrollahzadeh, J. Mol. Catal. A Chem. 383-384 (2014) 17.
- A. Roucoux, J. Schulz and H. Patin, Chem. Rev. 102 (2002) 3757.
- M. Nasrollahzadeh, S. M. Sajadi, A. Rostami-Vartooni, M. Khalaj, J. Mol. Catal. A Chem. 396 (2015) 31.
- M. Nasrollahzadeh, M. Maham, A. Ehsani and M. Khalaj, RSC Adv. 4 (2014) 19731.
- M. Nasrollahzadeh, M. Maham, M. M. Tohidi, J. Mol. Catal. A Chem. 391 (2014) 83.
- P. Fakhri, M. Nasrollahzadeh, B. Jaleh, RSC Adv. 4 (2014) 48691.
- M. Nasrollahzadeh, B. Jaleh, P. Fakhri, A. Zahraei, E. Ghadery, RSC Adv. 5 (2015) 2785.
- M. Alkan, M. Dogan, J. Colloid Interface Sci. 243 (2001) 280.
- N. Tekin, E. Kadıncı, O. Demirbas, M. Alkan, A. Kara, M. Dogan, Microporous Mesoporous Mater. 93 (2006) 125.

- M. Nasrollahzadeh, S. M. Sajadi and M. Khalaj, RSC Adv. 4 (2014) 47313.
- F. Halaweish, S. Kronberg and J. A. Rice, J. Chem. Ecol. 29(5) (2003) 1073.
- A.-F. M. RIZK, Bot. J. Linn. Soc. 94 (1987) 293.
- G. D. Manners and D. G. Davis, Phytochem. 23 (1984) 1059
- N. Ahmad, S. Sharma, Md. K. Alam, V. N. Singh, S. F. Shamsi, B. R. Mehta, A. Fatma, Colloids Surf. B. 81 (2010) 81.
- K. Tian, W.-J. Liu, H. Jiang, ACS Sustain. Chem. Eng. (2014) DOI: 10.1021/sc500646a.
- M. Nasrollahzadeh, S. M. Sajadi, M. Maham and A. Ehsani, RSC Adv. 5 (2015) 2562.
- M. Nasrollahzadeh, S. M. Sajadi, M. Maham, J. Mol. Catal. A Chem. 396 (2015) 297.
- M. Nasrollahzadeh, S. M. Sajadi, A. Rostami-Vartooni, M. Khalaj, RSC Adv. 4 (2014) 43477.
- M. Nasrollahzadeh, New J. Chem. 38 (2014) 5544.
- V. Mozaffarian, A Dictionary of Iranian Plant Names; Farhang Mo’aser, Tehran, 1996, p. 219.
- M. Nasrollahzadeh, S. M. Sajadi, M. Maham, P. Salaryan, A. Enayati, S. A. Sajjadi, K. Naderi, Chem. Nat. Compd. 47 (2011) 434.
- M.G. Mostafa, Y.-H Chen, J.-S. Jeanb, C.-C. Liu, Y-C Lee, J. Hazard. Mater. 187 (2011) 89.
- http://www.epa.gov/ttn/atw/hlthef/nitrophe.html.
- Y.-T. Woo and D. Y. Lai, Aromatic Amino and Nitro-Amino Compounds and Their Halogenated Derivatives. Patty’s Toxicology, Wiley, New York, 2001, pp. 1-96.
- A. K. Patra, A. Dutta and A. Bhaumik, Catal. Commun. 11 (2010) 651
- K. S. Shin, J. Y. Choi, C. S. Park, H. J. Jang, K. Kim, Catal. Lett. 133 (2009) 1
- S. Li, S. Guo, H. Yang, G. Gou, R. Ren, J. Li, Z. Dong, J. Jin, J. Ma, J. Hazard. Mat. 270 (2014) 11.
- Y. Choi, H. Son Bae, E. Seo, S. Jang, K. H. Park, B.-S. Kim, J. Mater. Chem. 21 (2011) 15431.
- R. Leary and A. Westwood, Carbon 49 (2011) 741.
- B. Sreedhar, D. K. Devi, D. Yada, Catal. Commun. 12 (2011) 1009.

- D. Shah, H. Kaur, J. Mol. Catal. A: Chem. 381 (2014) 70.
- K. Layek, M. L. Kantam, M. Shirai, D. Nishio-Hamane, T. Sasaki and H. Maheswaran, Green Chem. 14 (2012) 3164.
- R. J. Kalbasi, A. A. Nourbakhsh, F. Babaknezhad, Catal. Commun. 12 (2011) 955.
- C. Xu, Y. Yuan, R. Yuan and X. Fu, RSC Adv. 3 (2013) 18002.
- M. Xie, F. Zhang, Y. Long and J. Ma, RSC Adv. 3 (2013) 10329.
- Z. Duan, G. Ma, and W. Zhang, Bull. Korean Chem. Soc. 33 (2012) 4003.
- P. Wang, F. Zhang, Y. Long, M. Xie, R. Li and J. Ma, Catal. Sci. Technol. 3 (2013) 1618.
- M. Islam, P. Mondal, A. S. Roy, K. Tuhina, Transition Met. Chem. 35 (2010) 427.
- A. K. Shil, D. Sharma, N. R. Guha, P. Das, Tetrahedron Lett. 53 (2012) 4858.
- H. Yang, S. Li, X. Zhang, X. Wang, and J. Ma, J. Mater. Chem. A 2 (2014) 12060.
- Y. Choi, H. S. Bae, E. Seo, S. Jang, K. H. Park and B.-S. Kim, J. Mater. Chem. 21 (2011) 15431.
- J. Li, C.-Y. Liu and Y. Liu, J. Mater. Chem. 22 (2012) 8426.
- X. Wang, J. Fu, M. Wang, Y. Wang, Z. Chen, J. Zhang, J. Chen, Q. Xu, J. Mater. Sci. 49 (2014) 5056.
- Z. Dong, X. Le, X. Li, W. Zhang, C. Dong, J. Ma, Appl. Catal. B: Environ. 158-159 (2014) 129.
- P. Deka, R. C. Deka and P. Bharali, New J. Chem. 38 (2014) 1789.
- Z. Wang, C. Xu, G. Gao and X. Li, RSC Adv. 4 (2014) 13644.
- N. Sahiner, H. Ozay, O. Ozay, N. Aktas, Appl. Catal. A: Gen. 385 (2010) 201.
- N. Sahiner, Prog. Polym. Sci. 38 (2013) 1329.
- R. F. W. Bader, Atoms in Molecules, Oxford University, U.K., 1995.
- P. Popelier, Atoms in Molecules, Pearson, U.K., 2000.
- C. F. Matta, R. J. Boyd, The Quantum Theory of Atoms in Molecules, Wiley, Weinheim, 2007.